Expanded View Figures

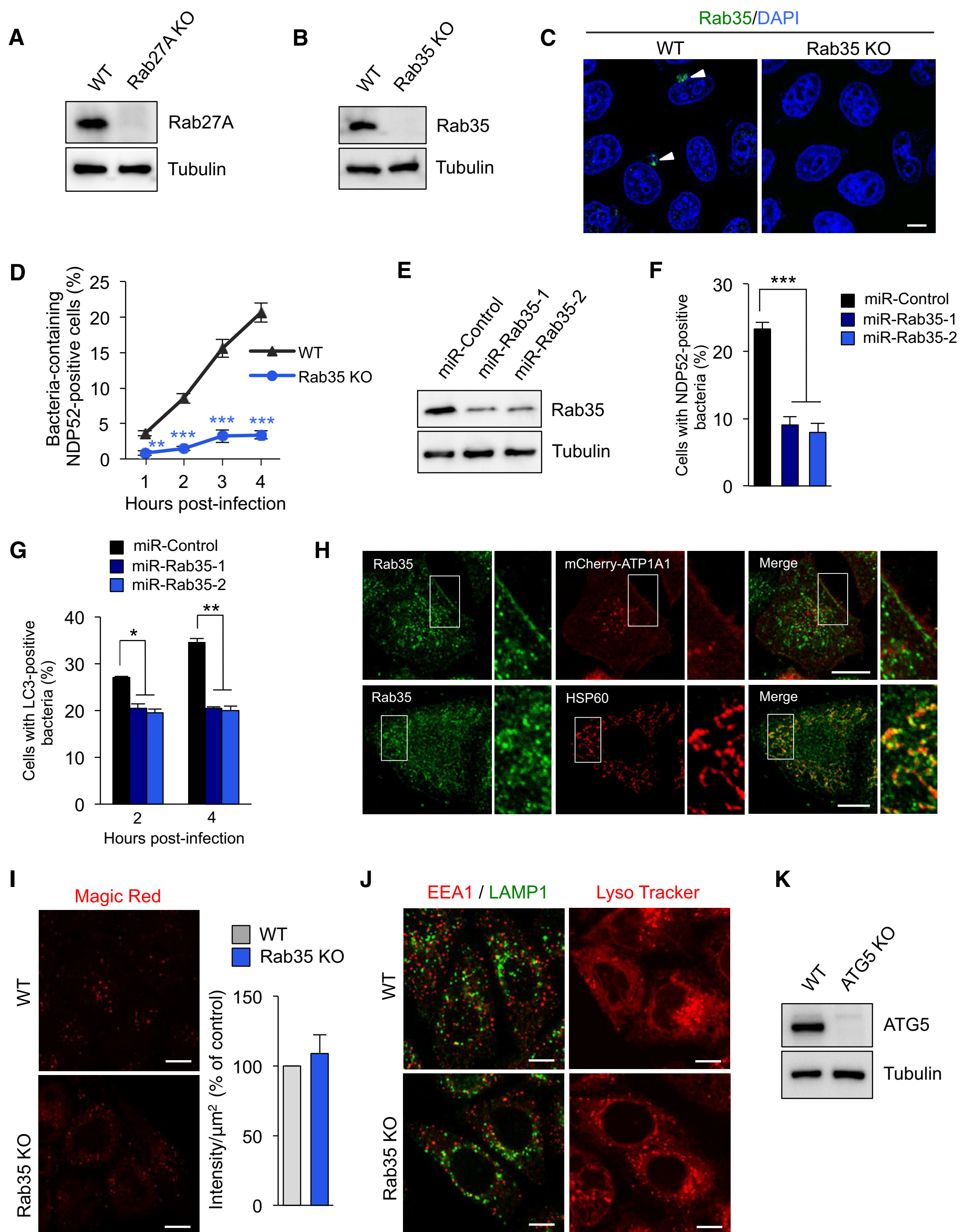

Figure EV1.

Figure EV1. Analysis of knockdown and knockout of Rab35.

A, B Knockout of Rab27 (A) and Rab35 (B) in HeLa cells.

C HeLa wild-type and Rab35 knockout cells were infected with GAS for 4 h, fixed, immunostained with anti-Rab35 antibody, and stained with DAPI. Arrowheads indicate Rab35-positive GAS.

D Time course of Rab35-dependent NDP52 recruitment to GAS. HeLa wild-type and Rab35 knockout cells expressing mCherry-NDP52 were infected with GAS. The percentages of cells with NDP52-positive GAS were quantified.

E miR-RNAi knockdown of Rab35.

F, G Control (miR-Control) and Rab35-knocked down (miR-Rab35) HeLa cells expressing mCherry-NDP52 (F) or mCherry-LC3 (G) were infected with GAS. Cells were analyzed with confocal microscopy and quantified the percentages of cells with NDP52-positive or LC3-positive GAS.

H Subcellular localization of endogenous Rab35.

I HeLa wild-type and Rab35 knockout cells were treated with Magic Red Cathepsin B (Magic Red CatB, in red) for 2 h. Quantification of the intensity of the Magic Red Cathepsin B signal, presented as a percentage of control (wild-type cells).

J Wild-type and Rab35 knockout HeLa cells were immunostained with against EEA1 and LAMP1 (left images) or treated with Lysotracker (100 nM) for 90 min (right images).

K Knockout of ATG5 in HeLa cells.

Data information: Data in (D, F, G, and I) are mean ± SEM from three independent experiments. Data were tested by two-tailed Student's *t*-test: *$P < 0.05$, **$P < 0.01$, ***$P < 0.001$. Scale bars, 10 μm.

© 2017 The Authors

Figure EV2. Effects of Rab35 mutants on autophagosome formation and recruitment of NDP52 to bacteria.

A, B Representative confocal micrographs (A) and autophagosome formation (B) in HeLa cells expressing mCherry-LC3 along with EmGFP, EmGFP-Rab35, EmGFP-Rab35 Q67A, or EmGFP-Rab35 S22N, infected for 4 h with GAS, and stained with DAPI.

C, D Representative confocal micrographs (C), and NDP52-tagged bacteria (D) in HeLa cells expressing mCherry-NDP52 along with EmGFP, EmGFP-Rab35, EmGFP-Rab35 Q67A, or EmGFP-Rab35 S22N, infected for 4 h with GAS, and stained with DAPI.

E Western blotting in HeLa wild-type and Rab35 knockout cells stably expressing EmGFP, EmGFP-Rab35, EmGFP-Rab35 Q67A, or EmGFP-Rab35 S22N.

F, G HeLa wild-type and Rab35 knockout cells stably expressing EmGFP, EmGFP-Rab35, EmGFP-Rab35 Q67A, or EmGFP-Rab35 S22N were transfected with mCherry-NDP52 and infected with GAS for 4 h. Confocal images (F) and quantification of NDP52 recruitment to GAS (G).

H HeLa wild-type and Rab35 knockout cells stably expressing EmGFP, EmGFP-Rab35, EmGFP-Rab35 Q67A, or EmGFP-Rab35 S22N were transfected with mCherry-LC3 and infected with GAS for 4 h.

Data information: Data in (B, D, G, and H) are mean ± SEM from three independent experiments. Data were tested by two-tailed Student's *t*-test: *$P < 0.05$, **$P < 0.01$, ***$P < 0.001$. Scale bars, 10 μm.

© 2017 The Authors

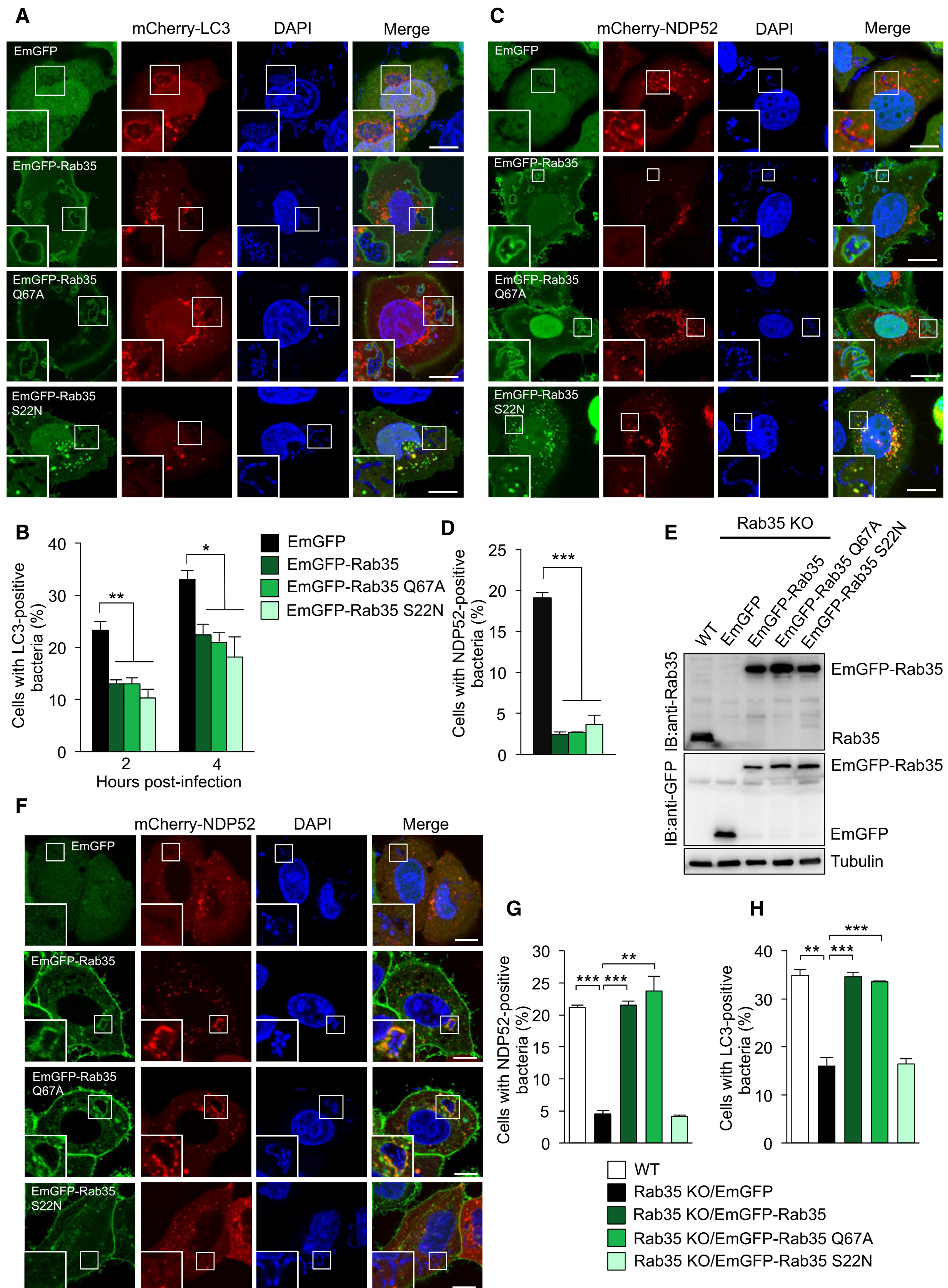

Figure EV2.

    © 2017 The Authors

Figure EV3. Involvement of Rab35 and TBC1D10A in NDP52 recruitment to damaged mitochondria.

A Confocal micrographs of mCherry-Rab35 recruited to depolarized mitochondria in HeLa wild-type (WT) and NDP52 knockout cells expressing EmGFP-Parkin, exposed to CCCP for 8 h, and immunostained with antibodies against mitochondrial TOM20.

B, C HeLa cells expressing EmGFP-Parkin along with mCherry-NDP52 treated with antimycin A (4 μM) and oligomycin (10 μM) for 8 h and immunostained with anti-TOM20. Representative confocal micrographs (B) and quantification (C) of NDP52 recruitment to mitochondria.

D HeLa cells were treated with CCCP for the indicated times and analyzed by Western blot against NDP52, Rab35, and actin.

E, F HeLa cells expressing EmGFP-Parkin, mCherry-NDP52, and FLAG, FLAG-TBC1D10A, or FLAG-TBC1D10A R160K were treated with antimycin A and oligomycin for 8 h, and immunostained with anti-TOM20 and anti-FLAG. Representative confocal micrographs (E) and quantification (F) of NDP52 recruitment to mitochondria.

Data information: Data in (C and F) are the mean ± SEM from three independent experiments. Data were tested by two-tailed Student's *t*-test: $***P < 0.001$. Scale bars, 10 μm.

© 2017 The Authors

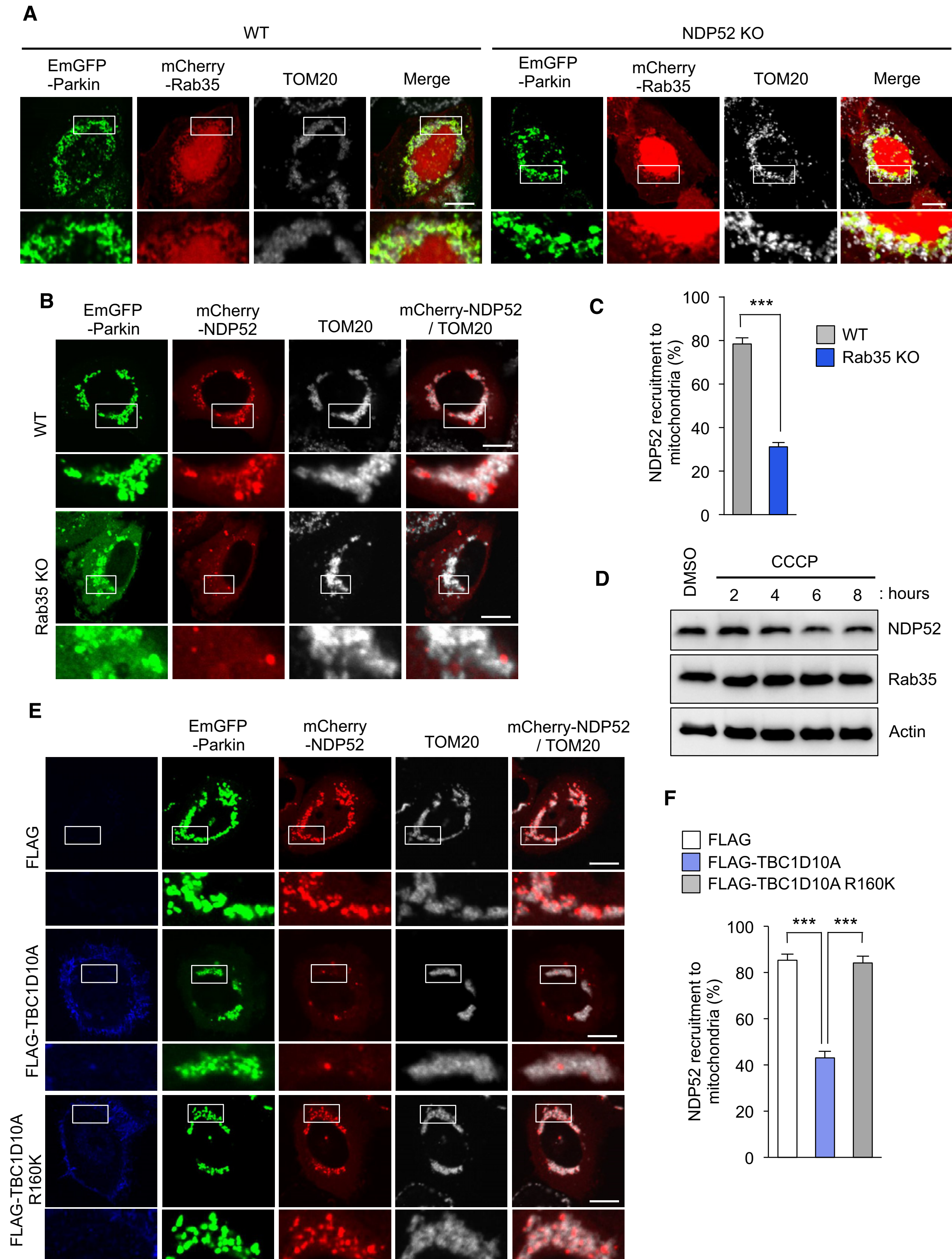

Figure EV3.

 © 2017 The Authors

Figure EV4. Recruitment of NDP52 to starvation-induced and basal autophagosomes.

A Confocal micrographs of autophagosomes in HeLa cells stably expressing GFP-LC3 along with mCherry-NDP52, mCherry-NDP52ΔCC, or mCherry-NDP52ΔZn, and cultured in regular (basal) or starvation medium for 2 h. Scale bars, 10 μm. Arrowheads indicate the NDP52-positive LC3 puncta.

B, C HeLa cells stably expressing GFP-LC3 along with FLAG, FLAG-TBC1D10A, or FLAG-TBC1D10A R1660K were cultured in regular (basal) or starvation medium for 2 h and immunostained for NDP52. Confocal images (B) and proportion of LC3 puncta colocalized with NDP52 from at least 30 randomly selected cells were quantified by Mander's coefficient M1 (C). Scale bars, 10 μm. Data were tested by two-tailed Student's *t*-test: $***P < 0.001$. Error bars indicate mean ± SEM.

© 2017 The Authors

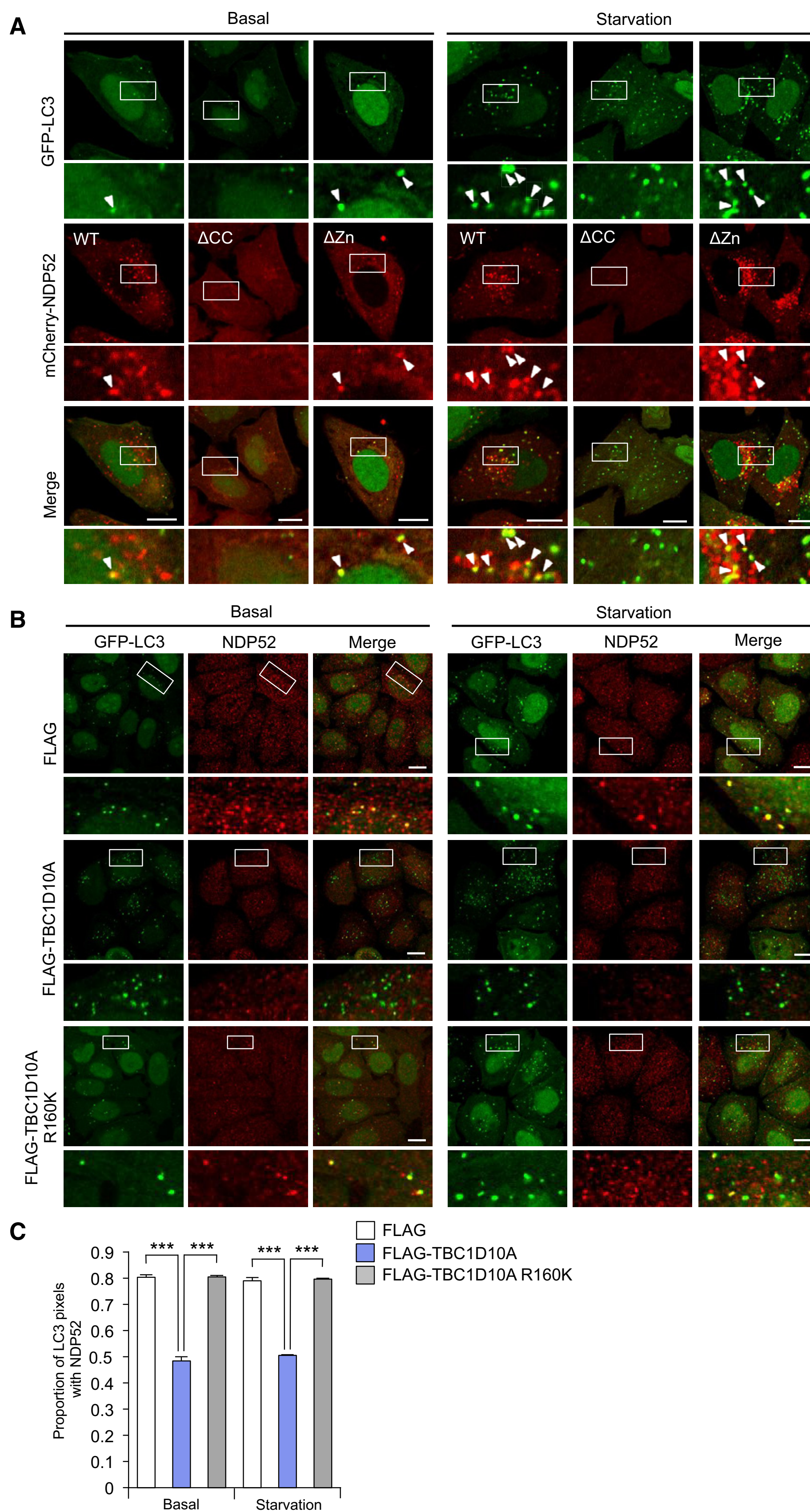

Figure EV4.

 © 2017 The Authors

Figure EV5. Rab35 localizes to bacteria-containing endosomes prior to membrane damage.

A HeLa cells were infected with GAS for 4 h and stained with anti-galectin 3 and anti-Rab35. Scale bars, 10 μm.

B Immunoelectron microscopy analysis revealed colloidal gold particles, indicating the presence of GFP-Rab35 around invading GAS. Scale bars, 0.5 μm.

C Live cell images of HeLa cells expressing EmGFP-Rab35 and mCherry-galectin 3, or mCherry-Rab35, and EmGFP-galectin 3 during GAS infection. Arrowheads indicate Rab35-positive GAS. Scale bars, 2 μm.

D, E HeLa cells expressed mCherry-NDP52 or-Rab35 were treated with DMSO or 4 μM BX795 for 24 h and infected with GAS for indicated times. The percentages of cells with NDP52 (D)- or Rab35 (E)-positive bacteria were quantified.

F, G HEK293T cells transfected with mKGN-NDP52 and mKGC-Rab35 or mKGN-NDP52ΔZn and mKGC-Rab35 were treated or untreated with BX795, and the green fluorescence was analyzed by microscopy. Representative micrographs (F) and quantification of fluorescence intensity (G). Scale bars, 10 μm. White lines indicate the outline of the cells.

Data information: Date in (D, E and G) were tested by two-tailed Student's *t*-test and error bars indicate the mean ± SEM from three independent experiments: $^{**}P < 0.01$, $^{***}P < 0.001$.

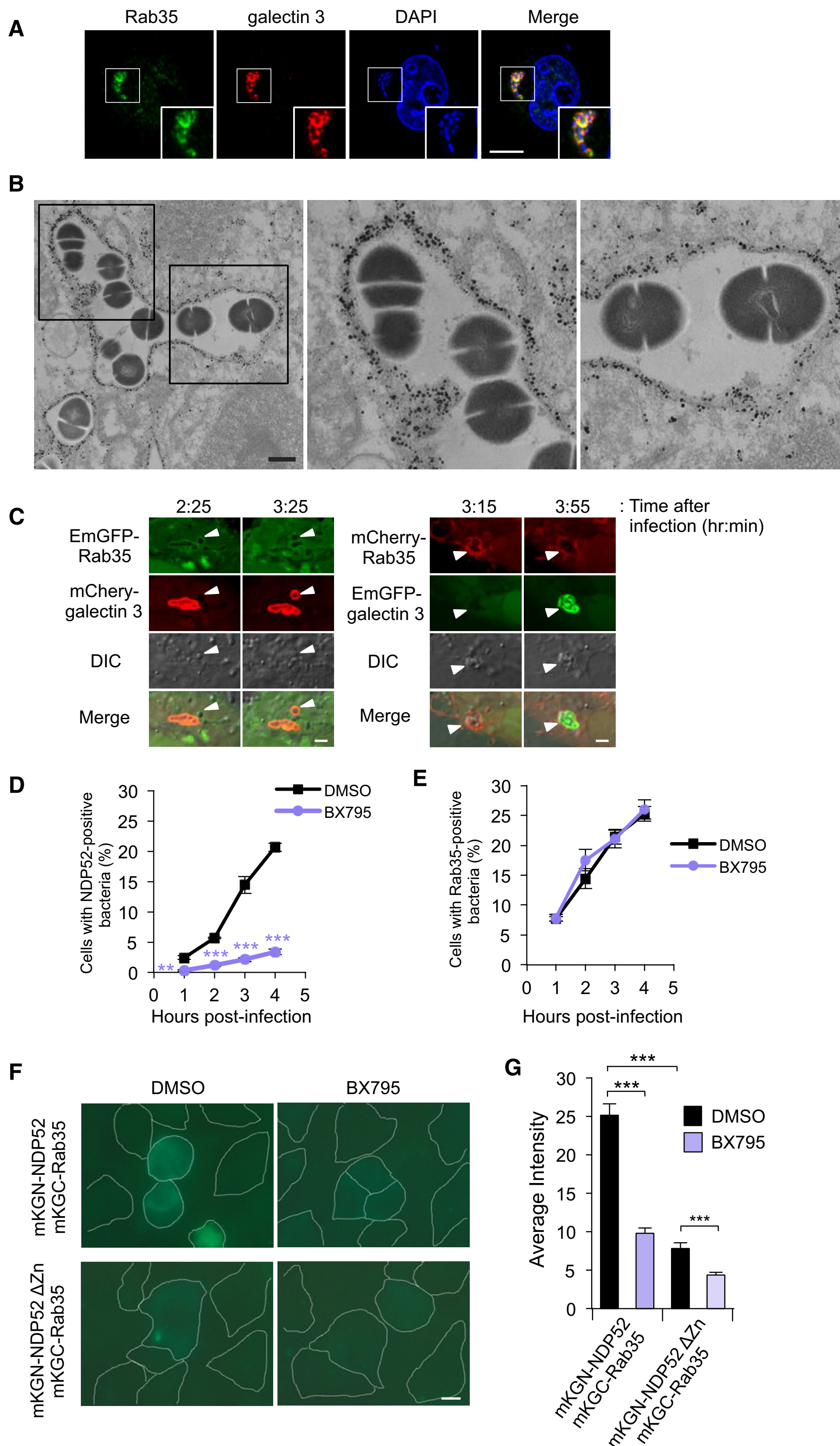

Figure EV5.

    © 2017 The Authors

Figure EV6. TBK1 regulates NDP52 recruitment to GAS and mitochondria by promoting Rab35-NDP52 interaction.

A Knockout of TBK1 in HeLa cells.

B Coimmunoprecipitation of endogenous Rab35 and NDP52 in wild-type or TBK1 knockout HeLa cells.

C, D HeLa cells expressed mCherry-NDP52 or-Rab35 were treated with DMSO or 4 μM BX795 for 24 h and infected with GAS for indicated times. The percentages of cells with NDP52 (C)- or Rab35 (D)-positive bacteria were quantified.

E Wild-type and TBK1 knockout HeLa cells expressed EmGFP-Parkin and either mCherry-NDP52 or -Rab35 were treated with 10 μM CCCP for 8 h. Cells were fixed and immunostained with antibody against TOM20.

F, G Wild-type and TBK1 knockout HeLa cells stably expressing mCherry-EmGFP-LC3 were cultured under starvation for 2 h. Representative confocal images (F) and quantification (G) of EmGFP-positive puncta.

H, I Wild-type and TBK1 knockout HeLa cells stably expressing GFP-LC3 were cultured under nutrient (basal) or starvation condition for 2 h. Cells were fixed and immunostained with an antibody against NDP52. Representative confocal micrographs (H) and proportion of LC3 puncta colocalized with NDP52 from at least 30 randomly selected fields were quantified by Mander's coefficient M1 (I).

Data information: Data in (C, D, G, and I) are the mean ± SEM from three independent experiments. Data were tested by two-tailed Student's *t*-test: *$P < 0.05$, **$P < 0.01$, ***$P < 0.001$. Scale bars, 10 μm.

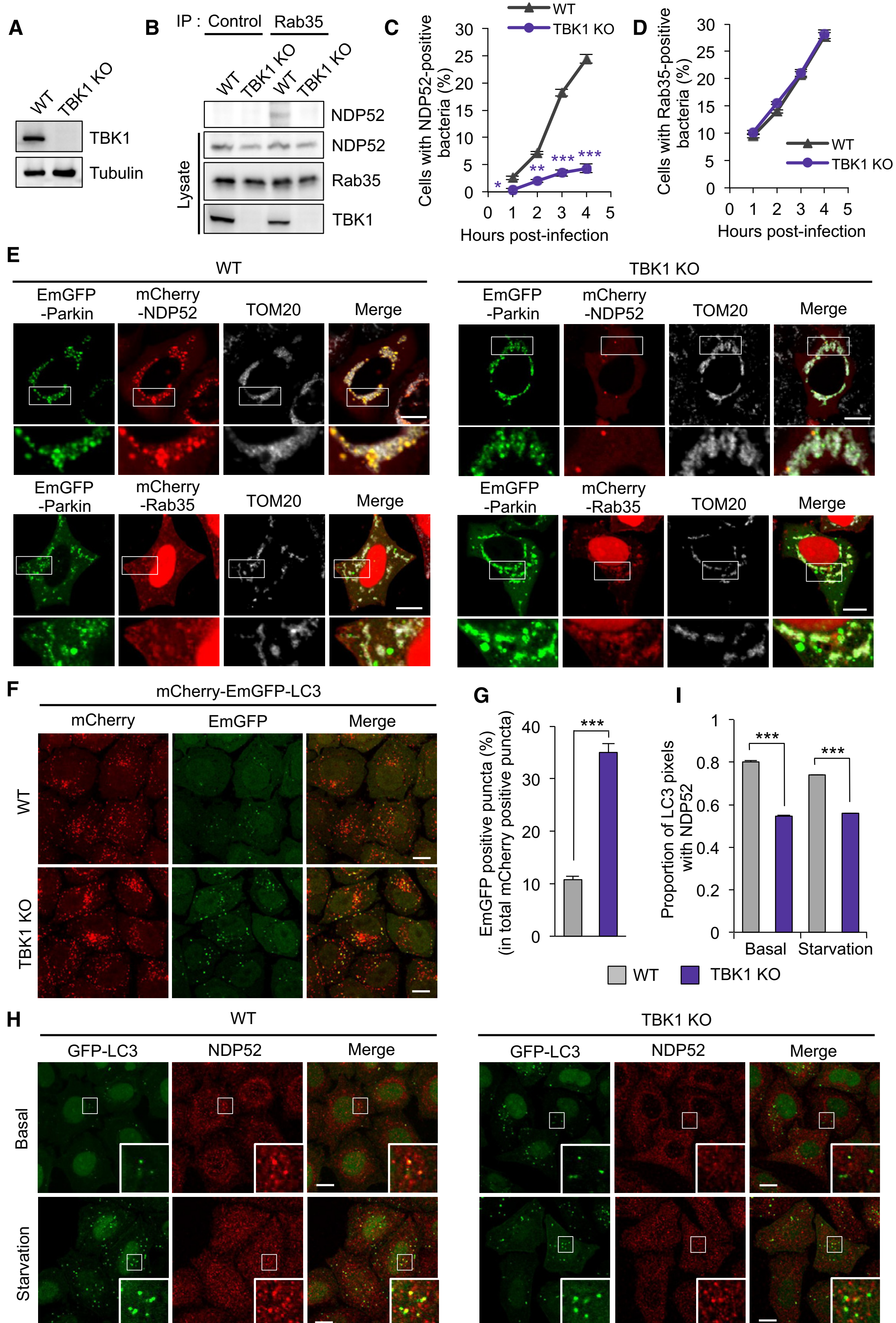

Figure EV6.

 © 2017 The Authors